electronics

MDPI

Article

Transformation of the Spatial Spectrum of Scattered Radio Waves in the Conductive Equatorial Ionosphere

Giorgi Jandieri [1,2] and Nika Tugushi [3,*]

[1] Department of Stochastic Analysis and Mathematical Simulation, Georgian Technical University, 0175 Tbilisi, Georgia; georgejandieri7@gmail.com
[2] Nanotechnology Centre, VSB—Technical University of Ostrava, 701 03 Ostrava, Czech Republic
[3] Department of Physics, Tbilisi State University, 0179 Tbilisi, Georgia
* Correspondence: tugushinika96@gmail.com; Tel.: +99-5598-228-086

Abstract: The oblique radio wave incidence on a turbulent equatorial conductive collision plasma layer is considered. The "Compensation Effect" has been discovered by us. A complex refractive index of the equatorial terrestrial ionosphere has been derived for the first time. Second-order statistical moments of the spatial power spectrum (SPS) of scattered radio waves are obtained for the first time using the WKB method, taking into account the asymmetry of the problem: the inclined incidence of the wave on a plasma boundary and the asymmetry of the magneto-ionic parameters. It was established for the first time that a certain direction exists along which the inclined incidence radio wave on a plasma layer and the anisotropy parameters of a magnetoplasma compensate each other. This result will have great practical application in communication. In this case, the SPS of scattered radio waves neither widens nor is its maximum displaced. The behavior of this spectrum versus distance propagated by radio waves in the conductive equatorial ionosphere is analyzed numerically for different penetration angles and anisotropy factors of asymmetric anisotropy electron density irregularities. It was shown that the anisotropy factor of elongated plasmonic structures has a substantial influence on the "Compensation Effect" of scattered ordinary and extraordinary waves penetrating in the conductive collision ionospheric plasma the slab. Numerical calculations are carried out for the anisotropic Gaussian correlation function applying IRI experimental data.

Keywords: turbulence; statistical moments; ionospheric plasma; conductivity; radio waves; ordinary and extraordinary waves; irregularities

Citation: Jandieri, G.; Tugushi, N. Transformation of the Spatial Spectrum of Scattered Radio Waves in the Conductive Equatorial Ionosphere. *Electronics* **2023**, *12*, 2759. https://doi.org/10.3390/electronics12132759

Academic Editor: Roald M. Tiggelaar

Received: 29 April 2023
Revised: 29 May 2023
Accepted: 12 June 2023
Published: 21 June 2023

1. Introduction

Randomly varying magneto-ionic plasma parameters containing electron concentration inhomogeneities have a significant impact on communication accuracy and navigation in a wide frequency band. Randomly varying plasma parameters have a substantial influence on the radio waves. Conductivity, collision between the plasma particles, complex refractive index, and its imaginary part cause significant impact on the statistical characteristics of scattered radio waves propagating in the conductive collision ionospheric magnetized (COCOIMA) plasma, particularly in the equatorial region of the terrestrial atmosphere. Asymmetry of the task can also lead to the increase in turbulence in magnetoplasma. The direction of both the geomagnetic field and an inclined incident of radio wave on a conductive turbulent collision magnetoplasma is a reason for the asymmetry of the problem. Inclined incident plane radio waves on the boundary of absorptive plasma layer penetrating into the turbulent plasma become inhomogeneous.

In many papers [1–4], second-order statistical characteristics of the multiple scattered radio waves in the terrestrial ionosphere have been investigated analytically and numerically using experimentally observed data. It was shown [5] that at small angles of incidence wave on a surface between vacuum and isotropic collisional turbulent plasma, the spatial (angular) power spectrum (SPS) of a multiple scattered radio wave monotonically

broadens with distance approaching a certain asymptotic value [5]. New phenomena arise increasing at increasing asymmetry of the problem: the incline incidence of radio waves on the anisotropic collision plasma slab. Different spectral components of the SPS attenuate variously; the width of the SPS anomalously broadens and becomes asymmetric with respect to its maximum. The peak of the SPS maximum is non-monotonically shifted to the normal relative to the interface between vacuum and collisional magnetoplasma. This is a consequence of the asymmetry of the task. Similar phenomena arise not only at the inclined incident wave on a surface; such anisotropy can also be an internal property of a turbulent plasma itself.

Turbulent conductive collisional magnetoplasma is a randomly inhomogeneous absorptive medium. The inclined incidence of a plane radio wave on a semi-infinite collision magnetoplasma layer with electron concentration fluctuations was considered [6–8] in a small-angle scattering approximation. Spectrum width varies nonmonotonically with distance from a plasma boundary. The widening of the SPS of scattered radio waves and shift of its maximum for both anisotropic Gaussian and power–law correlation spectral functions of electron concentration fluctuations in the turbulent collisional magnetoplasma were analyzed [7–9], applying the Wentzel–Kramers–Brilluen method. In this case, the width of the spectrum of a scattered electromagnetic wave substantially exceeds the width of the collisionless plasma. The "Compensation Effect" in the polar terrestrial ionosphere was considered in [10].

Physical processes in the polar and equatorial ionospheres are very different. Statistical moments of scattered radio waves propagating in the equatorial terrestrial ionosphere are investigated for the first time. They include the following anisotropy parameters: anisotropy of the ionosphere, taking into account Hall's, Pedersen, and longitudinal conductivity fluctuations, the direction of an external magnetic field, anisotropy of elongated plasmonic structures due to the diffusion processes in the filed aligned and field perpendicular directions containing anisotropy factor and the inclination angle of anisotropic ionospheric irregularities with respect to the geomagnetic lines of forces, incline incidence of wave on a turbulent plasma layer. A Complex refractive index of the equatorial terrestrial ionosphere has been obtained for the first time. Evaluation of the SPS of scattered electromagnetic waves propagating in the COCOIMA plasma is investigated in this paper using the complex ray-(optics) approximation. Compensation conditions are established for the experimentally observed power–law spectral function of electron density irregularities applying the statistical ionospheric model IRI.

2. Radio Wave Propagation in a Homogeneous Conductive Magnetized Plasma

The electric field satisfies the wave equation:

$$(\nabla_i \, \nabla_j - \Delta \, \delta_{i\,j} - k_0^2 \, \widetilde{\varepsilon}_{i\,j} \,) \, E_j(\mathbf{r}) = 0 \tag{1}$$

where: $k_0 = \omega/c$ is the wavenumber of an incident wave having frequency ω; Δ is the Laplacian, δ_{ij} is the Kronecker symbol, $\widetilde{\varepsilon}_{ij} = \varepsilon_{ij} - \, i \, \widetilde{\sigma}_{ij}$, $\widetilde{\sigma}_{ij} \equiv \sigma_{ij} \, (4\pi/k_0 \, c)$ are the second rank permittivity and conductivity tensors of the COCOIMA plasma, respectively.

Let a plane radio wave be incident from vacuum on a semi-infinite homogeneous COCOIMA magnetoplasma layer; Y axis coincides with an external homogeneous magnetic field $\mathbf{H_0}$. Conductive homogeneous collision magnetoplasma have permittivity tensor components:

$$\begin{gathered} \widetilde{\varepsilon}_{xx} = \widetilde{\varepsilon}_{zz} = \varepsilon_{\perp} - i \, \left(\sigma_{\perp} + s \, g \, \right), \, \widetilde{\varepsilon}_{xz} = - \, \widetilde{\varepsilon}_{zx} = - \, s \, \text{æ} \, \delta + i \, \left(\widetilde{\sigma}_H + \text{æ} \, \right), \\ \widetilde{\varepsilon}_{yy} = \varepsilon_{||} - i \, \left[\widetilde{\sigma}_{||} \, + s \, \left(g - p_0 \, u \, \, g_1 \right) \right], \, \widetilde{\varepsilon}_{xy} = \, - \widetilde{\varepsilon}_{yx} = \widetilde{\varepsilon}_{yz} = \widetilde{\varepsilon}_{zy} = 0 \end{gathered} \tag{2}$$

where $\varepsilon_{\perp} = 1 - p_0$, $p_0 = \text{v}/(1-u)$, $\text{æ} = p_0 \, \sqrt{u}$, $\varepsilon_{||} = 1 - \text{v}$, $\text{g} = p_0 \, (1+u)/(1-u)$, $\delta = 2/(1-u)$, $g_1 = (3-u)/(1-u)$, $s = \nu_{eff}/\omega$, $u = (e \, H_0/m_e \, c \, \omega)^2$, $\omega_p(\mathbf{r}) = \left[4 \, \pi \, n_e(\mathbf{r}) \, \, e^2/m_e\right]^{1/2}$ is the plasma frequency, $\text{v}(\mathbf{r}) = \omega_p^2(\mathbf{r})/\omega^2$, ν_{eff} is the ef-

fective collision frequency of electrons with other plasma particles, $n_e(\mathbf{r}) = n_0 + n_1(\mathbf{r})$ is the electron density, n_0 is a homogeneous background term, $n_1(\mathbf{r})$ is a random function of position, $n_1 << n_0$; e and m_e are charge and mass of an electron, respectively.

$$\sigma_\perp = e^2 N \left(\frac{\nu_e}{m_e\,(\nu_e^2 + \omega_e^2)} + \frac{\nu_i}{m_i\,(\nu_i^2 + \omega_i^2)} \right),$$

$$\sigma_H = e^2 N \left(\frac{\omega_e}{m_e\,(\nu_e^2 + \omega_e^2)} - \frac{\omega_i}{m_i\,(\nu_i^2 + \omega_i^2)} \right),$$

$$\sigma_{||} = e^2 N \left(\frac{1}{m_e\,\nu_e} + \frac{1}{m_i\,\nu_i} \right),$$

$\sigma_\perp$, σ_H, and $\sigma_{||}$ are the Pedersen, Hall's, and longitudinal conductivities, respectively, $\nu_{e\,,\,i}$ is the electron or ion collision frequency with the neutral molecules, $\omega_{\,e}$ and $\omega_{\,i}$ are an electronic and an ionic angular gyrofrequencies, respectively; $m_{\,e}$ and $m_{\,i}$ are the mass of an electron and an ion, respectively.

Equation (1) yields the set of equations for the COCOIMA plasma

$$\begin{aligned}
&(k^2\ \sin^2\theta\cos^2\varphi + k^2\cos^2\theta - k_0^2\,\widetilde{\varepsilon}_{xx})\ E_x - (k^2\sin^2\theta\sin\varphi\cos\varphi)\ E_y - \\
&- (k^2\sin\theta\cos\theta\sin\varphi + k_0^2\,\widetilde{\varepsilon}_{xz})\ E_y = 0, \\
&(k^2\sin^2\theta\sin\varphi\cos\varphi)\ E_x - (k^2\ \sin^2\theta\sin^2\varphi + k^2\cos^2\theta - k_0^2\,\widetilde{\varepsilon}_{yy})\ E_y + \\
&+ (k^2\sin\theta\cos\theta\cos\varphi)E_z = 0, \\
&(k^2\sin\theta\cos\theta\sin\varphi - k_0^2\,\widetilde{\varepsilon}_{xz})\ E_x + (k^2\sin\theta\cos\theta\cos\varphi)\ E_y - \\
&- (k^2\ \sin^2\theta\sin^2\varphi + k^2\sin^2\theta\cos^2\varphi - k_0^2\,\widetilde{\varepsilon}_{xx})\ E_z = 0
\end{aligned} \tag{3}$$

Here, φ is the polar angle between of the wave vector $\mathbf{k}$ on the XOZ plane.

If the directions of radio wave propagation and the homogeneous imposed magnetic field are perpendicular ($\theta = 90^0$) and $\varphi = 0^0$, we obtain two roots

$$k_I = k_0\,[\,(\varepsilon_\perp + æ + \sigma_H) - i\,\sigma_\perp\,]^{\,1/2} \text{ and } k_{II} = k_0\,[\,(\varepsilon_\perp - æ - \sigma_H) - i\,\sigma_\perp\,]^{\,1/2} \tag{4}$$

only the Hall's and Pedersen conductivities give the contribution in Equation (3), $E_y = 0$. Substitution (4) into (3) gives $(E_z/E_x) = \mp\, i$. Consequently, we have a right-hand circularly polarized (RHCP) wave (upper sign) and a left-hand circularly polarized (LHCP) wave (lower sign) propagating along the homogeneous magnetic field. Analyses show that $k_{II} < k_I$, the rotation is clockwise and, hence, the Faraday rotation angle is $\theta_F = (k_{II} - k_I)/2$. For an incident 3 MHz frequency wave, $\theta_F = 0.01$.

At quasi-longitudinal propagation of wave ($\theta = 0^0$), we have the following roots: $k_I = k_0\,\sqrt{m_1 + i\,m_2}$, $k_{II} = k_0\,\sqrt{\varepsilon_{yy}}$, where $m_1 = (\varepsilon_\perp\ t_0 + \sigma_\perp\ t_1)/(\varepsilon_\perp^2 + \sigma_\perp^2)$, $m_2 = (\sigma_\perp\ t_0 - \varepsilon_\perp\ t_1)/(\varepsilon_\perp^2 + \sigma_\perp^2)$, $t_1 = 2\ \varepsilon_\perp\ \sigma_\perp$, $t_0 = \varepsilon_\perp^2 - \sigma_\perp^2 - (æ + \sigma_H)^2$. Contrary to the previous case, the second root contains the longitudinal conductivity. For nonconductive plasma, $k_I = k_0\,\sqrt{(\varepsilon_\perp^2 - æ^2)/\varepsilon_\perp}$. The second root is the same.

Ionospheric plasma is an important subject of research in the field of radio physics for radio wave propagation. If θ is an angle between $\mathbf{H_0}||Y$ and $\mathbf{k}_0 \subset YOZ$ vectors, $s << \varepsilon_{i\,j}$, $\widetilde{\sigma}_{i\,j}$, complex refractive index of the conductive collision equatorial ionospheric plasma was obtained in [11].

After some transformations from Equation (1), we obtain

$$tg^2\theta = -\,\frac{\varepsilon_{yy}\,(N^2 - \varepsilon_L)\,(N^2 - \varepsilon_R)}{(N^2 - \varepsilon_{yy})(\varepsilon_{xx}\,N^2 - \varepsilon_R\,\varepsilon_L)} \tag{5}$$

where: $\varepsilon_R = \varepsilon_{xx} + i\ \varepsilon_{xz}, \varepsilon_L = \varepsilon_{xx} - i\ \varepsilon_{xz}$. Equation (5) has two zero and two poles, wherein each feature corresponds to one of four major waves (modes) that may exist in the plasma. These modes in the conductive equatorial plasma can be classified as follows:

(1) Propagation of wave perpendicular to the external magnetic field ($\theta = \pi/2$)

$$(a)\ N^2 = 1 - (v + \sigma_{||});\ \text{O-wave.} \tag{6}$$

$$(b)\ N^2 = \frac{\varepsilon_R\ \varepsilon_L}{\varepsilon_{xx}} = \varepsilon_\perp \left[1 - \frac{(æ + \sigma_H)}{\varepsilon_\perp^2 - \sigma_\perp^2}\right] - i\,\sigma_\perp \left[1 + \frac{(æ + \sigma_H)}{\varepsilon_\perp^2 - \sigma_\perp^2}\right];\ \text{E-wave.} \tag{7}$$

(2) Wave propagation along the external magnetic field $(\theta = 0)$

$$(a)\ N^2 = \varepsilon_R = \left[\left(1 - \frac{v}{1 - \sqrt{u}}\right) - \sigma_H\right] - i\,\sigma_\perp;\ \text{a RHCP spiral wave} \tag{8}$$

$$(b)\ N^2 = \varepsilon_L = \left[\left(1 - \frac{v}{1 + \sqrt{u}}\right) + \sigma_H\right] - i\,\sigma_\perp;\ \text{a LHCP spiral wave} \tag{9}$$

these are weakly dumping radio waves propagating in the equatorial terrestrial ionosphere. In the absence of an external magnetic field and in a non-conductive plasma nonconductivities $(\sigma_{ij} = 0)$, all waves are reduced to the ordinary wave. At intermediate angles between 0 and $\pi/2$, propagating waves will represent some combinations of these major waves.

Group velocities $\mathbf{v}_{gr}$ of both ordinary and extraordinary (O− and E−) waves generally do not coincide with the phase velocity $\mathbf{v}_{ph} = \omega\ \mathbf{k}/k^2$. The angle Θ between $\mathbf{v}_{gr}$ and $\mathbf{k}$ in a homogeneous medium, as is known, is determined by the relation [1–3]

$$tg\ \Theta_{1,2} = -\frac{1}{2\ N_{1,2}^2}\ \frac{\partial\ N_{1,2}^2}{\partial\ \theta} \tag{10}$$

At small angles θ (quasi-longitudinal propagation) $N_{1,2}$ has a simple form

$$\begin{aligned} N_{1,2} &= 1 - \frac{v}{1 \mp \sqrt{u}\ \cos\theta}, \\ tg\ \Theta_{1,2} &= \frac{\mp\, v\ \sqrt{u}\ \sin\theta}{2\ N_{1,2}^2\ (1 \mp\ \sqrt{u}\ \cos\theta\ )^{\,2}} \end{aligned} \tag{11}$$

Upper sign corresponds to the ordinary wave (O-wave), lower sign—to the extraordinary wave (E-wave). It is easy to make sure that the ratio $tg\ \Theta_1 /\ tg\ \Theta_2$ determined by the last ratio less than zero, i.e., the group velocities of the O−wave and E−wave deviate from the phase in opposite directions.

It can be concluded that at vertical sounding of the ionosphere, the areas of reflection of O−wave and E−wave are spaced apart in the horizontal direction. Calculations show that at vertical sounding of the ionosphere in both the southern and northern hemispheres, the trajectory of O−wave deviate from the vertical to the equator, and the E−wave in the opposite direction.

If radio waves propagate along the external magnetic field in the equatorial ionosphere, from Equations (8) and (9) we obtain

$$\omega_1^{(e)} = (1 - \sigma_H)\left\{\omega_p \sqrt{1 + \frac{1 - \sigma_H}{4}\ \frac{\Omega_e^2}{\omega_p^2}} - \frac{\Omega_e}{2}\right\} < \omega_p, \tag{12}$$

$$\omega_2^{(e)} = (1 + \sigma_H)\left\{\omega_p \sqrt{1 + \frac{1 - \sigma_H}{4}\ \frac{\Omega_e^2}{\omega_p^2}} + \frac{\Omega_e}{2}\right\} > \omega_p. \tag{13}$$

the RHCP waves are reflected in the ionosphere, while LHCP waves penetrating the ionospheric layers will propagate in the upper ionosphere; $\Omega_e = e\,H_0/m_e\,c$ is the electron gyrofrequency.

3. Statistical Moments of the Phase Fluctuations

The main theoretical tool describing short wavelength electromagnetic waves propagation in the terrestrial atmosphere is the ray theory. It is one of the most important methods among other asymptotic methods for a number of reasons: one of them is its simplicity and the possibility of obtaining an analytical solution for a wide range of problems that cannot be investigated by accurate or other asymptotic methods.

Let us introduce the Cartesian system of coordinates; a plane layer of a turbulent COCOIMA plasma is radiated by a plane radio wave, refracting at an angle θ_1 relative to the normal to this layer (it is related to the angle of incidence θ_i by Snell's law). This is the asymmetry of the problem. The thickness of a plasma layer is L. At the equatorial latitudes, the geomagnetic field is nearly horizontal; therefore, we will assume that the homogeneous magnetic field vector $\mathbf{H_0}$ is directed along the y-axis and the wave vector of an incident wave $\mathbf{k_0}$; both are located in the YOZ plane (the main plane). Rectangular components of a complex wave vector on the Y and Z coordinate axes in vacuum are purely real values: $k_{0z} = k_0\ \sin\theta_i$, $k_{y1} = k_0\ \cos\theta_i = \sqrt{k_0^2 - k_{0z}^2}$, particularly $\partial\, k_{y1}/\partial\, k_{0z} = -\,tg\,\theta_i$. Refracting at the interface vacuum–plasma, this wave becomes inhomogeneous, as it obeys the boundary conditions, the Z-projection of its wave vector remains real, but the Y-projection becomes complex $k_{y2} = \sqrt{k_0^2\,N^2 - k_{0z}^2}$. We assume that the characteristic spatial scale of electron concentration irregularities exceeds the wavelength of an incident wave $l >> \lambda$ and $L >> l$. This allows the use the ray-(optics) approximation for the investigation of statistical moments of a scattered radio wave field.

Electron concentration fluctuations in a plasma layer cause fluctuation of a scattered field in the observation point. At small-angle scattering in the ray-(optics) approximation, second-order statistical characteristics are determined by fluctuation of a complex phase $\varphi(\mathbf{r})$ [3] satisfying the eikonal equation $k^2 = k_0^2\,N^2$, $\mathbf{k}(\mathbf{r}) = -\,\nabla\,\varphi$ complex wave vector is a function of position. Complex refractive index of the COCOIMA plasma contains components of the wave vector $N^2(\mathbf{r}) = N^2(n(\mathbf{r}),\ k_x,\ k_z,\ \omega)$. The eikonal equation can be rewritten as [8]

$$(\mathbf{k}\cdot\nabla\,\mathbf{k}\,) - \frac{1}{2}\,k_0^2\,\frac{\partial\,N^2}{\partial\,\mathbf{k}_\perp}\,\nabla\,\mathbf{k} = \frac{1}{2}\,k_0^2\,\frac{\partial\,N^2}{\partial\,n}\,\nabla\,n, \tag{14}$$

where, $\mathbf{k}_\perp = \mathbf{k}_\perp\,(\mathbf{k}_x\ ,\ \mathbf{k}_z)$. We can use the following series expansions for the wave vector and the following phase: $\mathbf{k} = \mathbf{k_0} + \mathbf{k_1}(\mathbf{r}) + \cdots$, $\varphi = \varphi_0 + \varphi_1 + \cdots$ leading to the relationship for the phase fluctuation considering only first order small terms of electron density fluctuations n_1/n_0. After some algebraic transformations, we obtain

$$k_{0y}\,\frac{\partial\,\varphi_1}{\partial\,y} + \left[\,k_{0z} - \frac{1}{2}\,k_0^2\,\left.\frac{\partial\,N_0^2}{\partial\,k_{0z}}\right|_{k_{0x}=0}\right]\,\frac{\partial\,\varphi_1}{\partial\,z} = -\,\frac{1}{2}\,k_0^2\,\frac{\partial\,N_0^2}{\partial\,n_0}\,n_1. \tag{15}$$

integrating Equation (15) along the complex characteristics, taking into account that

$$\frac{\partial\,k_{y2}}{\partial\,k_{0z}} = -\frac{1}{k_{y2}}\left(k_{0z} - \frac{k_0^2}{2}\,\frac{\partial\,N^2}{\partial\,k_{0z}}\right) \equiv \Upsilon_1 + i\,\Upsilon_2. \tag{16}$$

$$\begin{aligned}\Upsilon_1 &= tg\,\theta - \frac{1}{2\cos^2\theta\,(\Gamma_0^2+\Gamma_1^2)}\,\left(\Gamma_0\,\frac{\partial\,\Gamma_0}{\partial\,\theta} + \Gamma_1\,\frac{\partial\,\Gamma_1}{\partial\,\theta},\right)\\ \Upsilon_2 &= \frac{1}{2\,\cos^2\theta\,(\Gamma_0^2+\Gamma_1^2)}\,\left(\Gamma_1\,\frac{\partial\,\Gamma_0}{\partial\,\theta} - \Gamma_0\,\frac{\partial\,\Gamma_1}{\partial\,\theta}\right)\end{aligned} \tag{17}$$

Here, θ is an angle between $\mathbf{H_0}$ and the wave vector of a refracted wave.

Irregularities in the equatorial ionosphere are highly field aligned, and therefore the spread of F turbulence is 2D. At some scale length the spectrum is anisotropic, i.e., the ionosphere is much more narrowly bounded vertically than horizontally.

Taking into account the boundary condition, $\varphi_1(z=0)=0$ and expand the function φ_1 in a two-dimensional Fourier integral; for the phase fluctuations, we obtain

$$\varphi_1(x,L,z)=\frac{\alpha}{k_y}\int\limits_{-\infty}^{\infty}\mathrm{d}k_x\int\limits_{-\infty}^{\infty}\mathrm{d}k_z\ \exp(ik_x x\ +\ ik_z\,z)\int\limits_{0}^{L}\mathrm{d}\xi\ n_1(\,k_x,\xi,k_z)\ \exp\left\{-\,ik_z\left(\frac{\partial k_{y2}}{\partial k_{0z}}\right)_0(L-\xi)\right\} \tag{18}$$

where, $\alpha\equiv-\,\frac{1}{2}\,k_0^2\,\frac{\partial\,N_0^2}{\partial\,n_0}$; for brevity, the index '0' will be omitted everywhere.

Phase fluctuations allow for the investigation of second order statistical characteristics of scattered radio waves. A transverse correlation function of the phase fluctuation may be easily obtained

$$V_\varphi(\rho_x,\ L,\ \rho_z)=\ 2\,\pi\ \frac{\alpha^2}{k_y^2}\int\limits_{-\infty}^{\infty}dk_x\int\limits_{-\infty}^{\infty}dk_z\ W_n(k_x,\Lambda_2\,k_z\,,\ k_z)\ \frac{1}{2\ \Lambda_1\,k_z}\,[1-\exp\,(-\,2\,\Lambda_1\,k_z\,L)\,]\cdot \\ \cdot\ \exp\,(ik_x\,\rho_x+ik_z\,\rho_z) \tag{19}$$

where, ρ_z and ρ_x are distances between observation points spaced apart at small distances in the main and perpendicular planes, $V_n(\mathbf{k})$ is the arbitrary correlation function of electron concentration fluctuations.

At strong fluctuations of the phase $<\varphi_1\varphi_1^*>>>1$, it can be assumed, as usual [3], that they are normally distributed. If the regular phase difference is negligible, the transverse correlation function of the complex field is described by the formula

$$V_E(\rho_x,\ L,\ \rho_z)=\ E_0^2\ \exp\big[\,ik_z\,\rho_z-2\,(\mathrm{Im}\,k_{y\,2})L\big]\ \exp\left(\frac{\partial\,V_\varphi}{\partial\,\rho_z}\,\rho_z+\frac{1}{2}\,\frac{\partial^2\,V_\varphi}{\partial\,\rho_z^2}\,\rho_z^2+\frac{1}{2}\,\frac{\partial^2\,V_\varphi}{\partial\,\rho_x^2}\,\rho_x^2\right) \tag{20}$$

all derivatives of the correlation function of the phase are taken at $\rho_x=\rho_z=0$. Using the 2D Fourier transformation, we obtain the APS having great practical importance. This statistical characteristic is the same as the ray intensity (brightness) in the radiation transport equation [3]

$$S(k_x,\ L,\ k_z)=S_0\ \exp\left\{-\frac{(k_z-\Delta\,k_z)^2}{2\ \ <k_z^2>}-\frac{k_x^2}{2\ \ <k_x^2>}\right\}, \tag{21}$$

$$\Delta k_z=\frac{2}{i}\frac{\partial V_\varphi}{\partial\rho_z},<k_z^2>=-\frac{\partial^2 V_\varphi}{\partial\rho_z^2},<k_x^2>=-\frac{\partial^2 V_\varphi}{\partial\rho_x^2}, \tag{22}$$

Second-order statistical characteristics $\Delta_z\equiv\Delta\,k_z$ describe the displacement of maximum of the SPS due to the random variation of electron density, $\Sigma_z\equiv<k_z^2>$ and $\Sigma_x\equiv<k_x^2>$ determines the broadening of the SPS in the YOZ and XOY planes, respectively.

Substituting (18) into Equation (22), we yield

$$\begin{aligned}\Sigma_x\ &=\ \int\limits_{-\infty}^{\infty}dk_x\int\limits_{-\infty}^{\infty}dk_z\ \frac{k_x^2}{k_z}\,W_n(k_x,\ \Upsilon_1\,k_z\,,\ k_z\,)\,\Xi\,(k_z),\\ \Sigma_z\ &=\ \int\limits_{-\infty}^{\infty}dk_x\int\limits_{-\infty}^{\infty}dk_z\,k_z\,W_n(k_x,\ \Upsilon_1\,k_z\,,\ k_z\,)\,\Xi\,(k_z),\\ \Delta_z\ &=\ \int\limits_{-\infty}^{\infty}dk_x\int\limits_{-\infty}^{\infty}dk_z\,W_n(k_x,\Upsilon_1\,k_z\,,\ k_z\,)\,\Xi\,(k_z),\\ \Xi\,(k_z)\ &=\ \frac{2\,\pi}{\Upsilon_2}\,\frac{\alpha^2}{k_y^2}\,[1-\exp\,(-\,2\Upsilon_2\,k_z\,L)].\end{aligned} \tag{23}$$

the double integrals depend only on the spatial spectrum of electron concentration fluctuations but not on the strength of the fluctuations. As it was mentioned above, the asymmetry of the problem includes all anisotropic parameters of the turbulent conductive magneto-

plasma and oblique incidence of the wave. Particularly (a) at inclined incidence wave on the isotropic absorptive plasma $\partial k_{y2}/\partial k_{0z} = -k_{0z}/k_{y2}$, $Y_2 = 0$; (b) at oblique incidence of the wave on a magnetoplasma slab, we can apply Formula (19). From these formulas, follow that anomalous broadening of the APS and shift of its maximum are clearly manifested at $Y_2\ k_z\ L > 1$. Taking into account that $\partial\ N^2/\partial\ k_z\ \sim \partial\ N^2/\partial\ \theta$, we can directly apply formula (5) differentiating by angle θ. From the Equations (18) and (24), follow that at $Y_2 = 0$ exists the compensation direction, along which the SPS neither broadens nor does its maximum shift. At different incident angles on a plasma layer, the SPS will anomalously broaden, but the mean value of the SPS will displace to the compensation direction, increasing distance travelling by radio wave in the equatorial region of the COCOIMA plasma.

4. Numerical Calculations

Artificial ionospheric inhomogeneities generating across the geomagnetic field have scales ranging from a meter up to more kilometers. The statistical ionospheric model IRI recommended by URSI as a basic model in the study and prediction of ionospheric propagation of radio waves [12,13] is the most proven technology for describing the spatial distribution of electron density in the equatorial ionosphere.

Observing the characteristic linear scale of electron density irregularities in F region of the equatorial ionosphere is in the range from 100 m to 10 km. Satellite experiments consistently observe a power law spectrum of plasmonic structures, with the spectral index in the interval -1 to -3.

Experimental observation of the equatorial ionospheric irregularities distribution was analyzed by GPS signals registering by ground-based radar stations and by Ionospheric Scintillation Monitors (ISM). Irregularities in the equatorial ionosphere have a bubbles form, created near the magnetic equator on the bottom side of the F2 layer, rising along the geomagnetic lines of forces. These bubbles are generated due to a Rayleigh–Taylor-like instability. Experimentally observing the phase spectral index p describes the strength of electron density irregularities. According to the ISM observations, index p is in the interval $2.5 \leq p \leq 3.5$. Experimental observations of the anisotropic electron density irregularities in the F-region of the ionosphere show that they have power–law spectrum with a power index p [14,15]. The 3D spectral function can be written as follows:

$$W_n(\mathbf{k}) = \frac{C_n^2}{(2\pi)^{3/2}} \frac{r_0^3 (k_0 r_0)^{(p-3)/2}}{\left(r_0\sqrt{k^2 + k_0^2}\right)^{p/2}} \frac{K_{p/2}\left(r_0\sqrt{k^2 + k_0^2}\right)}{K_{(p-3)/2}(k_0 r_0)},$$

where, C_n^2 is the mean-square deviation of electron density, $K_\nu(x)$ is McDonald function, r_0 is the inner scale of turbulence, $L_0 = 2\pi/k_0$ is the outer scale. In the interval $k_0\ r_0 << k\ r_0 << 1$ correlation function is described by the formula [14,15]:

$$W_n(\mathbf{k}) = \frac{\sigma_n^2}{(2\pi)^{3/2}} \frac{\Gamma(p/2)}{\Gamma\left[\ (p-3)/2\ \right]} \frac{k_0^{p-3}}{(k^2 + k_0^2)^{p/2}}, \tag{24}$$

where $\Gamma(x)$ is the gamma function.

In analytical calculations, we apply the power–law spectral function:

$$W_n(\mathbf{k}) = \frac{C_n^2}{8\ \pi^{5/2}} \frac{A_p\ l_{||}^3}{\chi^2\left[1 + l_\perp^2\ (k_x^2 + k_y^2) + l_{||}^2\ k_z^2\right]^{\ p/2}}. \tag{25}$$

where, $A_p = \Gamma(p/2)\ \ \Gamma[\ (5-p)/2\ ]\ \sin[(p-3)\ \pi/2]$, $\chi = l_{||}/l_\perp$ is the anisotropy factor—the ratio of longitudinal and transverse characteristic linear sizes of plasma irregularities. The shape of electron density irregularities has a spheroidal form due to diffusion processes

in the field align and field perpendicular directions. Small-scale plasmonic structures of the ionospheric F region are mainly field-aligned [16–19].

In numerical calculations, we used experimental data on ionospheric parameters for an altitude of 300 km [12,13].

Figure 1 illustrates the deviation of ray trajectories of both O- and E-waves (Δh in meters) relative to the direction connecting the source and the receiver versus the distance between observation points (in km-s) (see formula (12). This figure illustrates the phenomenon of the "fountain effect" of the O- and E-waves, which was revealed in the approximation of geometric optics. In the area of the geomagnetic equator, the geomagnetic field is almost parallel to the Earth's surface. A global empirical ionospheric model IRI (International Reference Ionosphere) was used in numerical calculations of the equatorial latitudes. The behavior of O- and E-waves in the equatorial region is different. In this region of the ionosphere, the plasma rises and gradually turns north in the northern hemisphere and south in the southern hemisphere, which is caused by an increase in the inclination of geomagnetic lines of forces on both sides of the geomagnetic equator. As a result, maxima (or crest) of electron concentration are formed on both sides of the geomagnetic equator, i.e., north and south crests of equatorial anomaly or crests corresponding to ordinary and unusual waves. This effect significantly affects the operation of radio communication, radio navigation, location, etc.

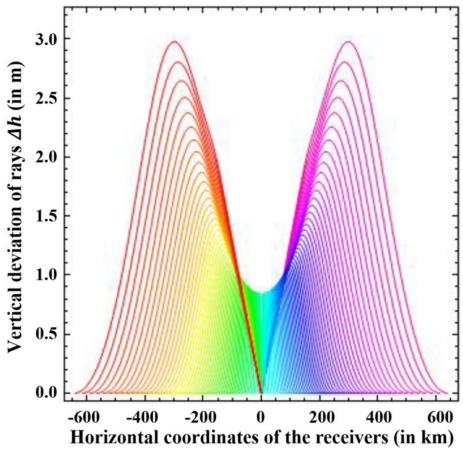

Figure 1. Relation of O- and E-waves ray paths deviation to observation points.

Figure 2 demonstrates the dependence of root mean square (RMS) deviation of the phase random variation versus the RMS deviation of electron concentration fluctuations. The phase spectral index p depends on the state of the ionosphere. In a calm ionosphere, parameter p varies within interval $1.7 \leq p \leq 2$, while in a highly perturbed ionosphere, the p value can increase to 4 and even to 6. At spectral index $p = 2$, the variance of the phase fluctuations of the received navigation radio signal is significantly less than at spectral index $p \geq 3$, and their difference increases in proportion to the RMS deviation of electronic concentration fluctuations in small-scale irregularities.

Figure 3 shows the 3D correlation function of the phase fluctuations as a function of distances between the observation points orthogonal (η_x) and parallel (η_y) to the magnetic field lines. Figure 4 illustrates the displacement of the maximum of the SPS of the O- (blue curves) and E-waves (red curves) in the conductive collision magnetized plasma at different penetration angle θ and anisotropy factor $\chi = 2$. SPS for the O-wave reaches maximums at $L/l_{||} = 49$, $\theta = 5^0$; and $L/l_{||} = 71$, $\theta = 15^0$. In this case, O-waves tend to the compensation direction at $L/l_{||} \approx 260$. SPS for E-wave has maxima at $L/l_{||} = 60$, $\theta = 10^0$; and $L/l_{||} = 51$, $\theta = 23^0$. The curves corresponding to E-wave reach the compensation direction at $L/l_{||} \approx 210$. The "Compensation Effect" of the displacement of the SPS for both waves takes place at a distance $L/l_{||} \approx 800$.

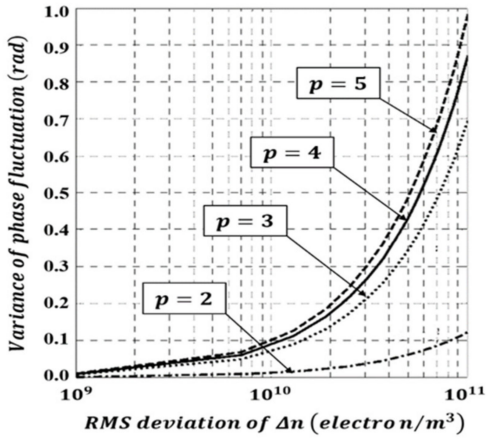

Figure 2. RMS deviation of $\sigma_{\varphi s}$ versus RMS deviation of σ_n for different phase spectral index p.

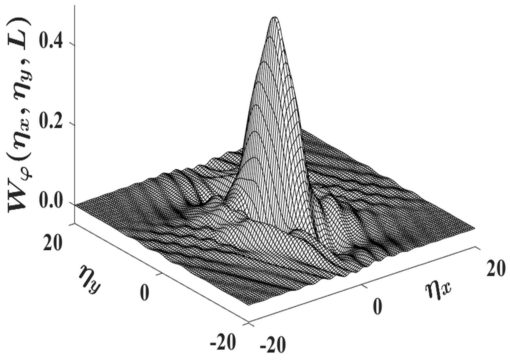

Figure 3. Three-dimensional correlation function of the phase fluctuations.

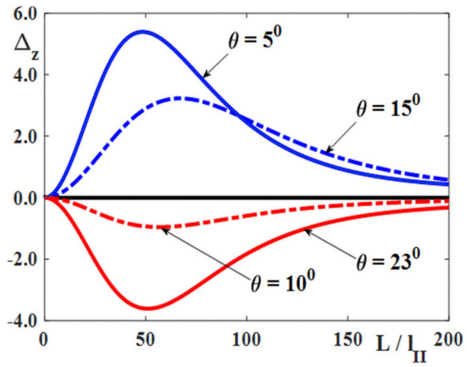

Figure 4. Shift of maximum of the SPS at non-dimensional space parameter.

Figure 5 shows the "Compensation Effect" for the broadening of both waves in the conductive equatorial terrestrial ionosphere at $\theta = 5^{\circ}$. The broadening of the SPS for O-wave in the main plane has a maximum at $\chi = 6$, propagating distance $L/l_{||} \approx 3.4 \cdot 10^3$; the broadening tends to the compensation direction at a distance $L/l_{||} \approx 8 \cdot 10^{3}$. For E-wave, the broadening of the SPS at the anisotropy factor $\chi = 6$ has a maximum at $L/l_{||} \approx 2.2 \cdot 10^3$ and tends to the compensation direction at $L/l_{||} \approx 10^{4}$. The "Compensation Effect" of the broadening of the SPS for E-waves is revealed earlier than for the O-waves. Figure 6 depicts the "Compensation Effect" for the broadening of both waves in the conductive equatorial region of the terrestrial ionosphere at $\theta = 20^{\circ}$. Broadening of the SPS corresponding to the O-wave reaches to the compensation direction at small anisotropy factor of electron density irregularities. The "Compensation Effect" for Σ_x is revealed at distance $L/l_{||} \approx 5 \cdot 10^3$ for O-wave. A varying anisotropy factor in the interval $\chi = 22 \div 25$, the "Compensation Effect" is observed at distances $L/l_{||} \approx 2 \cdot 10^{4}$.

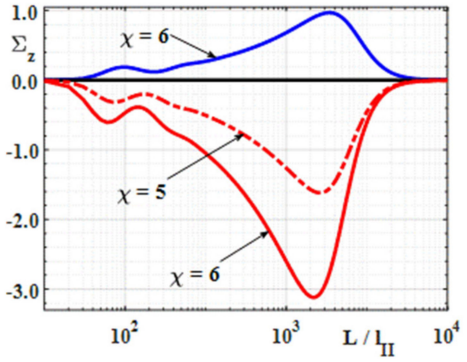

Figure 5. The broadening of the SPS versus non-dimensional spatial parameter in the main plane.

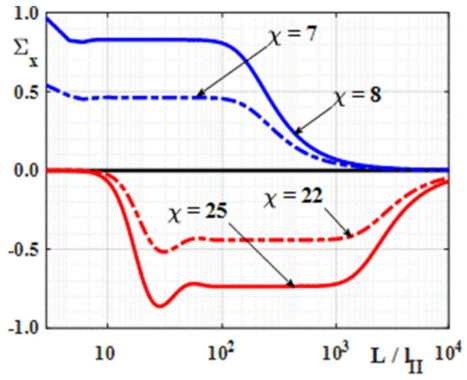

Figure 6. The broadening of the spectrum perpendicular to the main plane.

5. Conclusions

The statistical characteristics of the O- and E-radio waves are calculated, applying complex geometrical optics approximation. Anisotropy of the task contains inclined incidence of a radio wave on a plasma boundary, direction of the geomagnetic field, anisotropy of ionospheric conductivities: Hall's, Pedersen, and longitudinal conductivities, and anisotropy of ionospheric plasmonic structures.

A complex refractive index of the COCOIMA plasma of the equatorial region has been obtained for the first time. At radio waves propagation in a homogeneous conductive equatorial ionosphere, it is shown that there exist two weakly dumping RHCP and LHCP spiral-type waves containing Pedersen and Hall's conductivities. Calculating the Faraday angle, it was established that the rotation of the polarization plane is clockwise. The "fountain effect" of the O- and E-waves has been revealed. Crests corresponding to the O- and E-waves on both sides of the geomagnetic equator have been revealed.

Numerical analyzes were carried out for the experimentally observing anisotropic power–law spectral function of electron density fluctuations with the spectral index $p = 3$. Knowledge of the parameter p allow to determine anisotropy factor of elongated ionospheric irregularities measuring the backscattering cross-sections of radio waves with vertical and inclined soundings of the same ionospheric region $(\sigma_1/\sigma_2) \sim l_{||}^{1-p}$.

Asymmetry of the task: both the anisotropy factor of stretched electron density irregularities and ionospheric conductivities in the equatorial ionosphere play an important role in the "Compensation Effect"; particularly, they have significant influence on the E-wave. Radar sounding of the same area in the equatorial COCOIMA plasma at different frequencies and incidence angles makes it possible to define ionospheric parameters and the characteristic linear scales of elongated plasmonic structures. It was shown that at fixed anisotropy factor of elongated plasmonic structures and different penetration angles of O- and E-radio waves (asymmetry of the problem) in the COCOIMA plasma, the "Compensation Effect" takes place at small distances from a plasma boundary. At a fixed penetration

angle in the plasma slab, the varying anisotropy factor "Compensation Effect" appears at big distances from a plasma boundary in both main and perpendicular planes.

Investigating the features of electromagnetic waves propagation in the equatorial ionosphere allows to solve the problems of radio communication, radio navigation, as well as the problems of diagnosing of anisotropic ionospheric plasmonic structures.

Author Contributions: Conceptualization, G.J.; Methodology, G.J.; Software, N.T.; Investigation, G.J.; Data curation, G.J.; Writing—Original draft, G.J.; Visualization, N.T. All authors have read and agreed to the published version of the manuscript.

Funding: This work was supported by Shota Rustaveli National Science Foundation of Georgia (SRNSFG), grant NFR-21-316 "Investigation of the statistical characteristics of scattered electromagnetic waves in the terrestrial atmosphere and application".

Institutional Review Board Statement: Not applicable.

Informed Consent Statement: Not applicable.

Conflicts of Interest: The authors declare no conflict of interest.

References

1. Gershman, B.N.; Erukhimov, L.M.; Yashin, Y.A. *Wavy Phenomena in the Ionosphere and Cosmic Plasma*; Nauka: Moscow, Russia, 1984. (In Russian)
2. Kravtsov, Y.A.; Feizulin, Y.A.; Vinogradov, A.G. *Radio Waves Propagation through the Earth's Atmosphere*; Radio and Communication: Moscow, Russia, 1983. (In Russian)
3. Rytov, S.M.; Kravtsov, Y.A.; Tatarskii, V.I. Principles of Statistical Radiophysics. In *Waves Propagation Through Random Media*; Springer: Berlin, Germany; New York, NY, USA, 1989; Volume 4.
4. Ishimaru, A. Wave Propagation and Scattering in Random Media. In *Multiple Scattering, Turbulence, Rough Surfaces and Remote Sensing*; IEEE Press: Piscataway, NJ, USA, 1997; Volume 2.
5. Dolin, L.S.; Levin, I.M. *Handbook of Theory for Underwater Vision*; Gidrometeoizdat: Leningrad, Russia, 1991. (In Russian)
6. Gavrilenko, V.G.; Petrov, S.S. Correlation characteristics of waves in lossy media with smooth fluctuations of the refractive index with oblique incidence on boundary. *Waves Random Media* **1992**, *2*, 273–287. [CrossRef]
7. Aistov, A.V.; Gavrilenko, V.G.; Jandieri, G.V. On the influence of magnetic field on the angular power spectrum of electromagnetic wave multiply scattered in turbulent collisional magnetized plasma. *Izv. VUZ-Ov Radiofiz.* **1999**, *42*, 1165–1171. (In Russian) [CrossRef]
8. Jandieri, G.V.; Gavrilenko, V.G.; Semerikov, A.A. On the effect of absorption on multiple wave-scattering in a magnetized turbulent plasma. *Waves Random Media* **1999**, *9*, 427–440.
9. Jandieri, G.V.; Ishimaru, A.; Jandieri, V.G.; Khantadze, A.G.; Diasamidze, Z.M. Model computations of angular power spectra for anisotropic absorptive turbulent magnetized plasma. *PIER* **2007**, *70*, 307–328. [CrossRef]
10. Jandieri, G.; Ishimaru, A.; Mchedlishvili, N. Compensation effect in the conductive auroral regions of the terrestrial atmosphere. *PIER M* **2021**, *105*, 119–129. [CrossRef]
11. Jandieri, G.; Tugushi, N. Statistical characteristics of the temporal spectrum of scattered radiation in the equatorial ionosphere. *J. Environ. Earth Sci.* **2023**, *5*, 85–94. [CrossRef]
12. Bilitsa, D. International Reference Ionosphere 2000. *Radio Sci.* **2001**, *36*, 261–275. [CrossRef]
13. Bilitza, D.; Altadill, D.; Truhlik, V.; Shubin, V.; Galkin, I.; Reinisch, B.; Huang, X. International Reference Ionosphere 2016: From ionospheric climate to real time weather predictions. *Space Weather* **2017**, *15*, 418–429. [CrossRef]
14. Shkarofsky, I.P. Generalized turbulence space-correlation and wave-number spectrum-function pairs. *Can. J. Phys.* **1968**, *46*, 2133–2153. [CrossRef]
15. Kung, C.Y.; Liu, C.-H. Radio wave scintillations in the ionosphere. *IEEE Proc.* **1982**, *70*, 324–360. [CrossRef]
16. Fejer, B.G.; Kelley, M.C. Ionospheric irregularities. *Rev. Geophys. Space Phys.* **1980**, *18*, 401–454. [CrossRef]
17. LaBelle, J.; Kelley, M.C. The generation of kilometer scale irregularities in equatorial spread F. *J. Geophys. Res.* **1986**, *91*, 5504–5512. [CrossRef]
18. Cervera, M.A.; Thomas, R.M. Latitudinal and temporal variation of equatorial ionospheric irregularities determined from GPS scintillation observations. *Ann. Geophys.* **2006**, *24*, 3329–3341. [CrossRef]
19. Liu, Y.; Zhou, C.; Xu, T.; Tang, Q.; Deng, Z.; Chen, G.; Wang, Z. Review of ionospheric irregularities and ionospheric electrodynamic coupling in the middle latitude region. *Earth Planet. Phys.* **2021**, *5*, 462–482. [CrossRef]